Early Tissue Reaction at the Interface of Immediately Loaded Dental Implants

Ulrich Meyer, MD, DMD, PhD[1]/Hans-Peter Wiesmann, Phys[1]/
Thomas Fillies, MD, DMD[2]/Ulrich Joos, MD, DMD, PhD[3]

Purpose: *The treatment of patients with early or immediately loaded dental implants has renewed interest in the behavior of osteoblasts at the implant surface under load. A newly designed dental implant indicated for immediate loading was tested in vivo for early stages of osteoblast behavior at the implant surface.* ***Materials and Methods:*** *Thirty-two implants were placed in the mandibles of 8 minipigs. Half of the implants (n = 16) were immediately loaded under occlusal contacts, and implants placed in non-occlusal relations served as a control.* ***Results:*** *All implants, except 1 that showed signs of tissue infection, healed uneventfully and were stable throughout the experimental period. Ultrastructural analysis of mandibular specimens revealed an intimate attachment of osteoblasts to the material surface beginning as early as day 1. Application of either occlusal or non-occlusal load did not alter the phenotypic morphology of the attached osteoblasts. Transmission electron microscopy and x-ray diffraction analysis demonstrated a direct contact of bone-like minerals over the whole implant surface with no signs of crestal hard tissue alteration. Electron diffraction analysis showed a slight release of titanium from the implant side.* ***Discussion:*** *These results indicate that immediate loading of specially designed dental implants can be performed without disruption of the titanium/bone interface or disturbance of osteoblast physiology in the early loading phase.* ***Conclusion:*** *Immediate loading protocols can be performed without disturbance of normal bone biology.* (Int J Oral Maxillofac Implants 2003;18:489–499)

Key words: *bone formation, dental implants, finite element analysis, immediate loading, osteoblast*

The long-term success of osseointegrated implants in the treatment of completely and partially edentulous patients with a sufficient amount and quality of bone has been well documented in the literature.[1–3] It has generally been thought in implant dentistry that osseointegration requires a healing period of at least 3 months in the mandible and 5 to 6 months in the maxilla.[4–7] The rationale for choosing a delayed loading period was that premature loading resulted in fibrous tissue encapsulation rather than direct bone apposition.[7,8] It has been hypothesized that necrotic bone at the implant bed border is not capable of load bearing and should first be replaced by new bone.[4,7,9] Roberts and coworkers assumed that rapid remodeling of the dead bone layer compromises the strength of the osseous tissue supporting the bone-implant interface and that the integrity of the periosteal margin may be threatened by undermining of the remodeling process of adjacent bone during the healing period.[10,11] The release of material particles is another factor that has been suggested to impair bone physiology in the early remodeling stage.[12,13]

Therefore, experimental work was performed to investigate the hypothesis that osseointegration can be achieved when healing occurs under mechanical

[1]Assistant Professor, Department of Cranio-Maxillofacial Surgery, University of Münster, Münster, Germany.
[2]Resident, Department of Cranio-Maxillofacial Surgery, University of Münster, Münster, Germany.
[3]Director and Head, Department of Cranio-Maxillofacial Surgery, University of Münster, Münster, Germany.

Reprint requests: PD Dr Dr Ulrich Meyer, Department of Cranio-Maxillofacial Surgery, University of Münster, Waldeyerstr. 30, D-48149 Münster, Germany. Fax: +49-251-83-47-203. E-mail: ulmeyer@uni-muenster.de

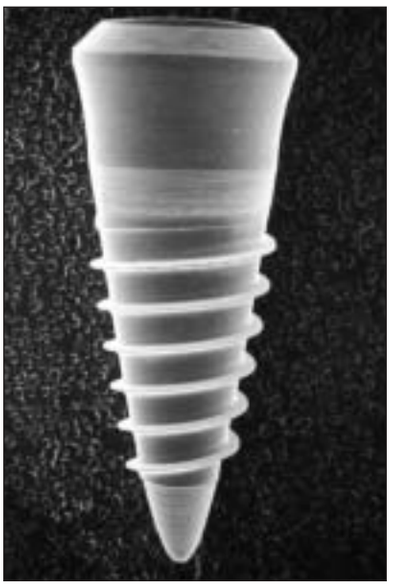

Fig 1a *(Left)* SEM of the implant used in this study (length 10 mm, shoulder diameter 4.1 mm). Microgrooves were located at the shoulder and tip of the implant.

Fig 1b *(Below)* Finite element model of strain distribution under vertical load. The model corresponds to the implant and bone anatomy at the implant site.

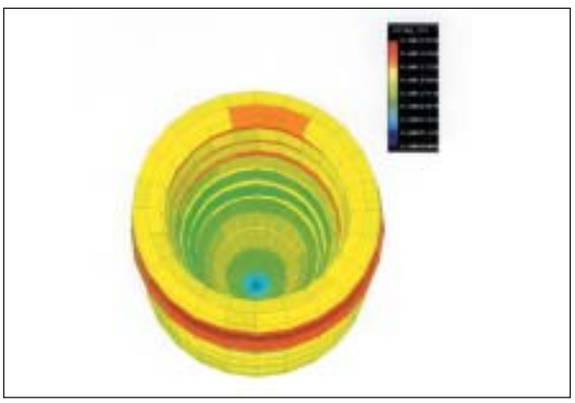

load. This issue has been addressed by several authors,[14–21] and a review of such evidence was given by Szmukler-Moncler and associates.[22] In addition, retrieved human samples of immediately loaded implants[18,20,23] substantiate the hypothesis that osseointegration can be achieved. Recent studies have indicated that although premature loading has been interpreted as inducing fibrous tissue interposition, immediate loading per se is not necessarily responsible for fibrous encapsulation. It is the excess of micromotion during the healing phase that interferes with bone repair.

At present, much is known about the impact of loading on peri-implant bone.[24–27] Some in vivo studies have indicated that load over a certain threshold may cause marginal bone loss[28,29] or even loss of implants,[30,31] while others have suggested that certain loads may increase the amount of mineralized bone at the interface and in the peri-implant bone.[10,32–34] Recent research has confirmed that the impact of loading on bone depends on motion in the microenvironment of the bone tissue. Lanyon demonstrated that bone remodeling results from strains in the microenvironment of bone tissue.[35] It has been shown that bone remodeling and collagen mineralization are directly related to the strains applied.[36] Frost proposed a minimum effective strain (500 με) necessary for bone maintenance from hyperphysiologic strains (> 4,000 με) leading to long-term bone failure.[37] Strain is defined as the relative elongation of cells and is calculated by the ratio between the initial cell length and the final length obtained. Therefore, the aim of this study was to investigate early osteoblast reactions at titanium implants designed to elicit homogeneous physiologic strains at the implant surface. Special emphasis was placed on the ultrastructural features of osteoblasts and the extent of mineral formation at early stages of cell/implant interactions under different loading conditions.

MATERIALS AND METHODS

Implant Design

The implants used in this study were newly developed conical screw-type implants with a length of 10 mm and a diameter of 4.1 mm at the shoulder of the implant (Fig 1a). The implants were made of pure titanium with a characteristic progressive thread design. The threads, as well as the curvature of the implant, provided a homogeneous strain distribution[38] over the whole implant surface under vertical loading conditions (Fig 1b). A numeric model was generated as a guideline for micromotion assessment under masticatory load. The gross morphology of the implants was designed with the help of finite element analysis (FEA). For these calculations, the exact size of the implant placement and the anatomy of the mandible were taken into account (Fig 2a). Previous investigations using FE models demonstrated that such an implant design leads to micromovement of a magnitude of 2,000 to 3,000 με in the bone layer adjacent to the implant surface (boundary conditions: 300 N vertical load, normal bone density, direct implant/bone contact).[39,40] Microgrooves (depth 20 μm, width 40 μm) were created at the bottom and shoulder of the

Fig 2a Three-dimensional computed tomogram of the skull. Bony dimensions at the implantation site approximated the bone anatomy modeled in the FEA model.

Fig 2b Scheme of implant placement. The distal implant was placed under occlusal contact and the mesial implant under non-occlusal contact.

Fig 2c Alveolar specimen after 14 days of load application.

Fig 2d Probe processing by separation of the sample with a blade.

implant to allow for osteoblast ingrowth. Cell cultures of osteoblasts were carried out as previously described.[41]

Experimental Animals

Eight male Göttinger minipigs, 14 to 16 months of age and with an average body weight of 35 kg, were used in this study. Minipigs were selected to ensure adequate alveolar ridge size and height for implant placement.[42] Both second premolars of the porcine mandible were extracted, and the extraction sites were allowed to heal for 3 months before implant placement. A total of 32 implants were placed into the mandibles of the minipigs. In accordance with the experimental design, 2 treatment groups were tested in each animal: 2 immediately loaded implants (test group) placed in occlusal contact (second premolar position) and 2 implants (control group) placed in a non-occlusal relation (primate gap) (Fig 2b). This study was approved by the Animal Ethics Committee of the University of Münster under the reference number G 90/99.

Surgical Procedure

All surgery was performed under sterile conditions in a veterinary operating theater. The animals were sedated with an intramuscular injection of ketamine (10 mg/kg), atropine (0.06 mL/kg), and stresnil (0.03 mL/kg). Tooth debris and calculus of the residual dentition were systematically removed before implant placement. A mucosa punch was used to expose the bone area, and bone sockets were made with a bur using continuous external sterile saline irrigation to minimize bone damage caused by overheating. Bone preparation was carried out with standard instruments provided in the implant kit according to the manufacturer's instructions for placement of 10-mm-long implants. The screw-type implants were carefully placed by manual tapping until they were fully embedded in the bone. After placement, the shoulder of each implant was 1 mm below the ridge crest to allow circumferential bone growth. Healing caps were inserted to allow soft tissue healing. Special care was taken to load implants vertically by a 1-point contact and to avoid transversal overload. The occlusion was tested by

occlusal foil and, if necessary, refined by a diamond bur.

The animals were inspected after the first few postoperative days for signs of wound dehiscence or infection and weekly thereafter to assess general health. A systematic oral health care regimen was performed during the experimental period. The minipigs were fed a normal diet. On days 1, 3, 7, and 14 of implant loading, 2 animals each were sacrificed with an overdose of T61 given intravenously. Following euthanasia, mandibular block specimens containing the implants and surrounding tissues were dissected from all of the animals. The block samples were sectioned by a saw to remove unnecessary portions of bone and soft tissue (Fig 2c). Block samples containing the implants were first divided into 2 halves, and then each sample was further dissected with a blade (Fig 2d) to obtain a sample containing the implant embedded in the alveolar bone and the corresponding bone sample detached from the implant. Samples containing the implant were used for scanning electron microscopic (SEM) investigations, whereas the bone sections without implant were prepared for element analysis, transmission electron microscopy (TEM), and electron diffraction analysis.

SEM and TEM

For TEM, samples were harvested adjacent to the shoulder, the body, and the tip of the implant. Tissue samples were fixed in 100 mmol/L phosphate buffer containing 2.5% glutaraldehyde (pH 7.4). Specimens were dehydrated in a graded series of alcohols and embedded in Araldite resin (EB Sciences, Agawam, MA), and ultrathin sections of about 80 nm were cut. The sections were stained for 1 hour with 2% uranyl acetate followed by incubation in Reynold's lead citrate for 10 minutes. Sections were examined under a Philips CM10 electron microscope (Amsterdam, The Netherlands) with an acceleration voltage of 60 kV.

For SEM, glutaraldehyde-fixed specimens were critical point–dried. Additionally, samples were fixed in liquid nitrogen–cooled propane and cryodried at –80°C. Samples were sputter-coated with gold for histologic analysis and with carbon for element determination. Specimens were examined under a field-emission SEM (LEO 1530 VP, Oberkochen, Germany) equipped with an EDX analyzer (Ince Energy 200, Oxford, United Kingdom). Because of the technical problems involved in assessing the mineralization process after chemical fixation, cryofixed specimens were prepared.[43] Element analysis was performed in the bone layer adjacent to the bone/implant interface.

Electron Diffraction Analysis

Electron diffraction analysis was carried out with a Philips CM10 transmission electron microscope using an acceleration voltage of 80 kV. For diffraction analysis, ultrathin sections were used. The contact time of the ultrathin sections with the water in the microtome was reduced to only a few seconds to avoid dissolution of the crystals. Three positions from each implant were used to investigate the mineral formation.

RESULTS

Clinical and Histologic Results

All but 1 of the implants healed uneventfully. At placement and during loading, the implants remained clinically immobile. One implant showed signs of soft tissue infection related to a gingival dehiscence occurring on day 3 after surgery. This implant was, therefore, not considered in the analysis. All implants were anchored monocortically. Dissection of the implant-containing bone by a blade confirmed the clinical finding that the implants were osseointegrated. There was intimate bone contact over the whole length of the implant (Fig 3a). Typically, endosteal bone covered the implant surface. Collagen fibers and osteoblasts made up the bulk of the adjacent tissue layer, and the collagen fibers appeared to be predominantly oriented perpendicular to the implant surface in the bulk bony tissue (Fig 3b). Cells, extracellular matrix proteins, and mineralized bone tissue were in direct contact with the implant (Fig 3c). In contrast to the collagen fibers in the original bone, which were oriented perpendicular to the implant, newly synthesized collagen in the vicinity of the surface appeared to form a felt-like matrix parallel to the surface.

The histologic appearance of the occlusal loaded implants (Figs 3a to 3c) and non-occlusal loaded implants (Figs 3d to 3f) was comparable. Intimate bone contact was present at the necks of implants. Bone was interspersed in the microgrooves at the shoulders and tips of the implants (Fig 3d). Typically, the cells were able to accommodate their whole cell bodies in the microgrooves (Figs 3e and 3f). Probe processing by sample fracturing for the electron microscopic investigations suggested that the bond between the implant and the adjacent bone layer seemed to mimic the bond in the bone tissue itself. On the implant surface, cells and extracellular matrix remained attached following separation from the enveloping bone (Figs 3b to 3f).

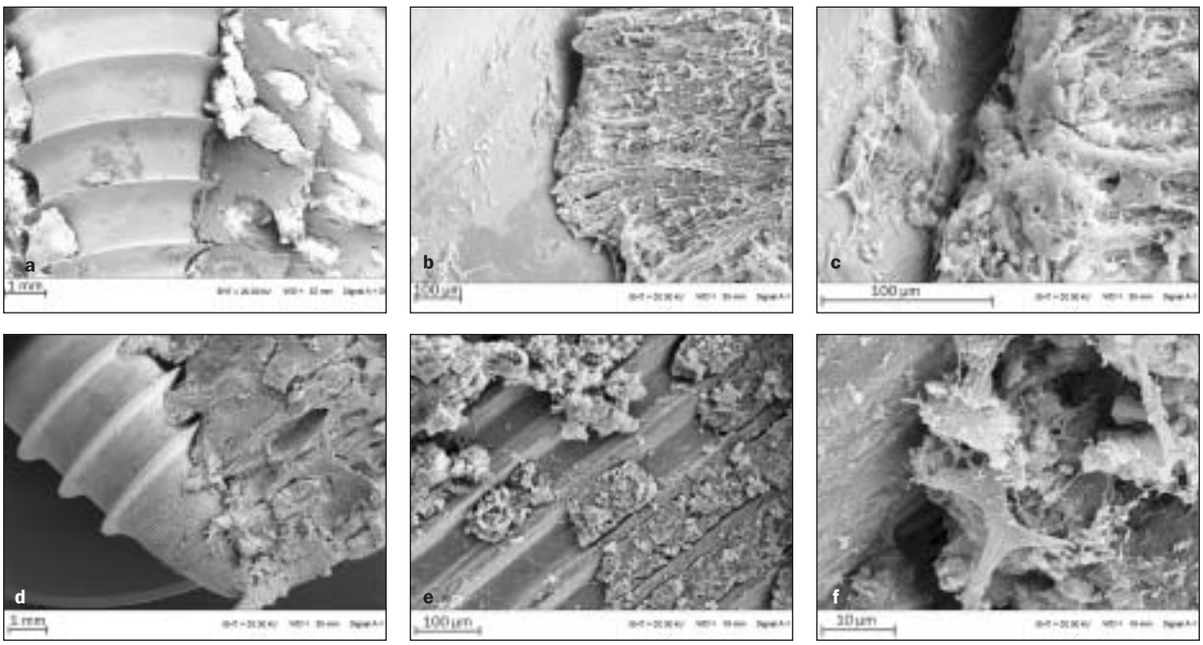

Figs 3a to 3f SEMs of implantation sites in porcine mandibular specimens at different magnifications. Bone-implant interfaces are shown after 14 days of occlusal (Figs 3a to 3c) or non-occlusal loading (Figs 3d to 3f).

Figs 4a and 4b SEMs of early osteoblast adhesion (a) at the implant surface and (b) on a polystyrene surface under cell culture conditions. Seeded cells were cultured for 24 hours. Cell culture experiments were performed as described by Meyer and coworkers.[41]

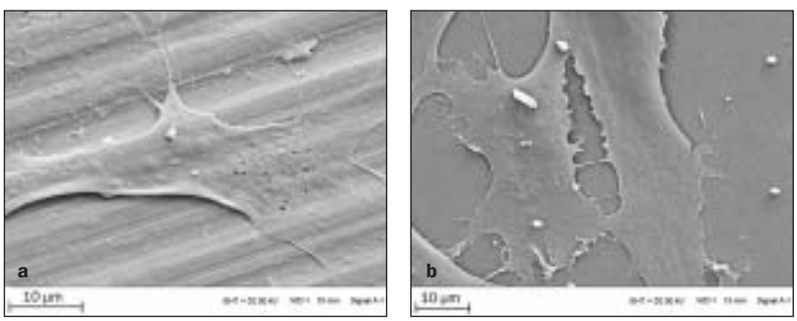

Cell Adhesion

SEM examinations revealed the stable attachment of osteoblasts spread over the implant surface. Osteoblasts at implant surfaces maintained their typical morphology. Figure 4a shows a monolayer of osteoblasts seeded onto the implant surface under cell culture conditions, while cells attached to polystyrene served as a control (Fig 4b). Immunohistochemistry of cells at the implant surface demonstrated the synthesis of osteocalcin and osteonectin, indicating the differentiated state of cells. Because of the smooth implant surface, most cells expressed a flattened morphology, which was seen also in the samples harvested from the porcine mandibles. Cells produced extracellular matrix proteins and remained in intimate contact with the implant (Fig 5a). A firm attachment of osteoblasts to the underlying implant surface was observed and was evident at higher magnifications. The cells usually exhibited a flat and polygonal configuration, in an apparent attempt to spread their cell body over the underlying surface. From the beginning of occlusal loading, cells attached directly to the titanium surface (Fig 5b) via cell extensions surrounded by extracellular matrix proteins. The surface of the implant was coated with a network of proteins (Fig 5c). Some of the red blood cells were extravasated and attached to the proteins at the implant surface. At the implant surface, extracellular fibrils (Fig 5c) with an organization suggestive of a collagenous matrix were observed. No difference was found between cell adhesion to the implants in the test and control groups. A disruption between the titanium surface and the cell/matrix layer was not observed.

Fig 5a SEM of cell morphology on day 3 of load application in porcine mandibular bone.

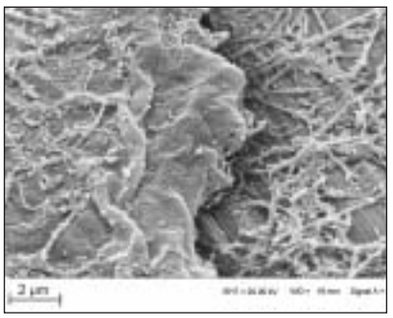

Fig 5b Extracellular matrix deposition resembled collagen assembly at the titanium surface.

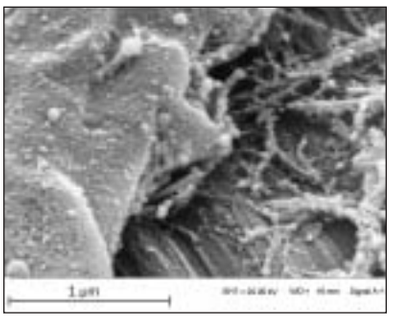

Fig 5c An intimate bond between the cell and the implant was visible at higher magnifications.

Figs 6a to 6f *TEMs of the interfacial area (day 3 of occlusal load application).*

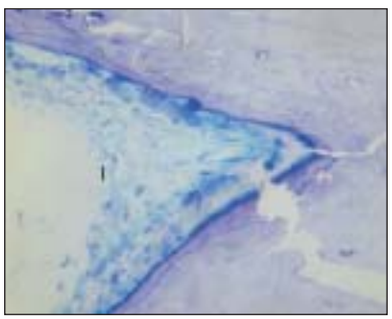

Fig 6a Semithin section of the bone layer adjacent to the implant shoulder. I = implant.

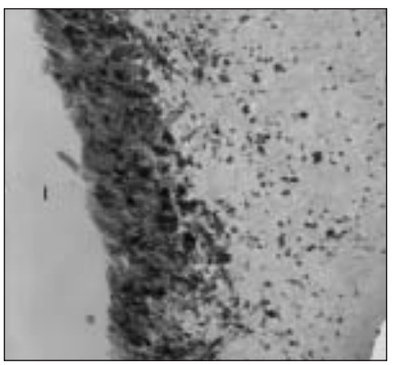

FIg 6b Extracellular mineral formation (magnification ×3,000). I = implant.

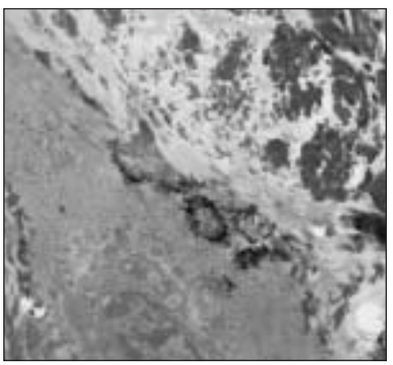

Fig 6c Ultrastructure of an osteoblast in the layer adjacent to the implant surface (magnification ×6,300).

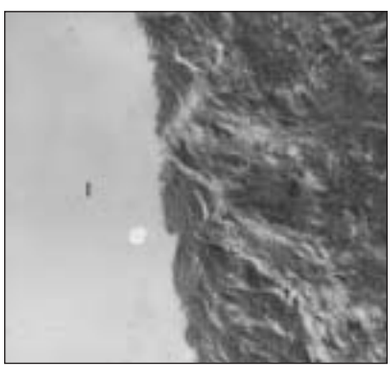

Fig 6d Unstained section of collagen mineralization at the implant surface (magnification ×6,300). I = implant.

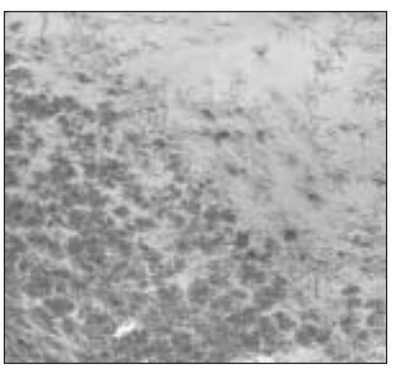

Fig 6e Unstained section of collagen mineralization in the microenvironment of the implant (magnification ×6,300).

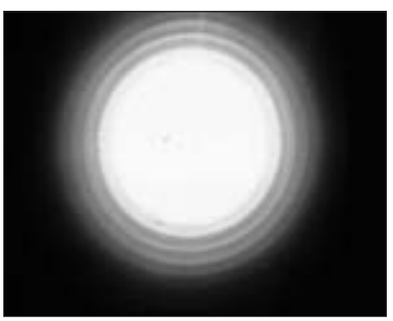

Fig 6f Electron diffraction pattern of mineral formation adjacent to the implant surface.

Patterns of Matrix Mineralization

In all bone samples, collagen fibers made up the bulk of the extracellular space, as judged by TEM. The assembly of collagen bundles seemed to be directed predominantly toward the implant surface. In specimens obtained from the implant surface, cells were embedded in a mineralized collagen-rich extracellular matrix (Figs 6a and 6b). Osteoblasts located adjacent to the implant surface displayed all signs of active cell function, including multiple mitochondria and an extended rough endoplasmic reticulum (Fig 6c). Figures 6d and 6e show characteristic TEM features and electron diffraction analysis patterns of mandibular specimens obtained directly from the implant neck (Fig 6d) or the adjacent tissue layer (Fig 6e). There was mature crystal

Figs 7a to 7c EDX analysis of element composition in the bone layer adjacent to the implant surface.

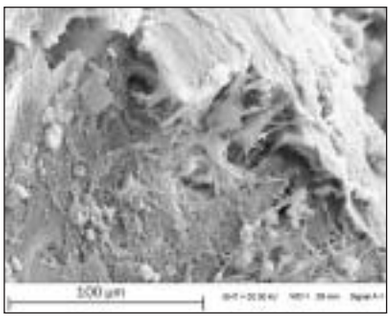

Fig 7a Tissue morphology after implant removal.

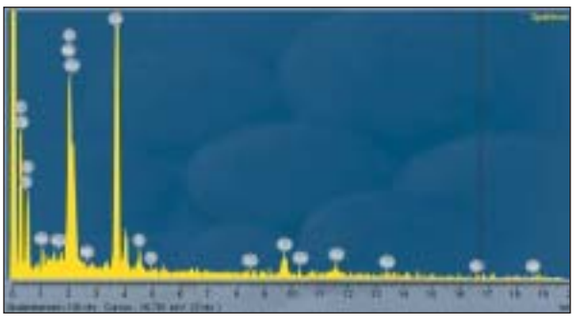

Fig 7b Element composition as determined over the image area (corresponding to Fig 7a).

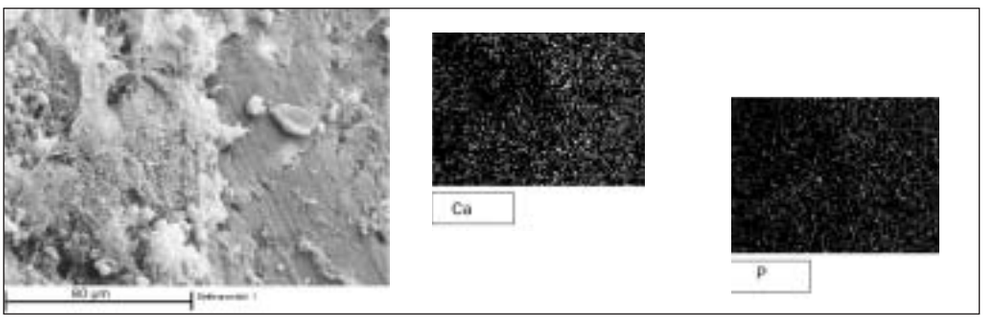

Fig 7c SEM and element distribution at higher resolution. The element distribution corresponded to the scanning electron micrograph on the left. Cellular elements as well as mineralized extracellular matrix were visible at the surface.

formation at the implant surface (Fig 6f), as detected by a typical diffraction pattern. No difference in the extent and nature of mineral formation was seen between the test and control groups. On an ultrastructural level, minerals displayed features of complete extracellular matrix mineralization over the whole experimental period at the entire implant surface (shoulder, body, tip). In search of titanium particles in the tissue layer adjacent to the implant surface, the authors found only a slight release of titanium from the implant (Figs 7a to 7c). High resolution of tissue morphology and element distributions in the layer adjacent to the implant confirmed that cells and mineralized extracellular matrix components at the implant surface lacked the presence of morphologically detectable titanium particles (Fig 7c). The ratio of calcium and phosphorus reflected the composition of hydroxyapatite in the bony tissue (Fig 7b).

DISCUSSION

Insights into cellular processes occurring at the implant/bone interface have contributed much to an understanding of biocompatibility and will provide a challenge to produce biomaterials with specific and desired biologic responses.[44,45] In this study, a dental implant that was engineered to maintain normal osteoblast physiology and mineral deposition at the implant surface under load was used. Given a primary bond between the implant material and the bony tissue, masticatory forces can be transmitted directly to the underlying bone, thereby preventing bone deformations that could result in adverse motions between the implant and the bone. The implant used in this study was designed to have a homogeneous and physiologic strain distribution (1,000 to 4,000 με) over the whole implant surface under a vertical occlusal load of 300 N. Some assumptions and limitations have been made in this FE model with regard to the material properties and model generation.[39,40] Bone tissue (cortical and trabecular bone) was assigned uniform isotropic elastic properties, although in vivo, bone probably exhibits a more complex situation. A number of in vitro studies including FEA have reported peak stress and strain magnitudes to occur in the marginal peri-implant bone after peak load applications.[46–50] It is tempting to extrapolate these findings to explain peri-implant bone loss in vivo. FEA used for the assessment of strains in the

microenvironment of bone is based on assumptions that may not describe the in vitro strains accurately in a mathematical sense. However, it has been previously demonstrated by in vivo strain gauge measurements that FEA is, in principle, suitable for the measurement of strain magnitudes under mechanical loading.[51,52]

The behavior of osteoblasts and mineral formation at implant surfaces has been studied by various groups, with the main focus on the biocompatibility of these materials. However, these materials have only rarely been subjected to mechanical loading, and there is some debate as to the tolerable amount of strain and the mechanical factors that govern the process of bone remodeling. Research on bone formation in orthopedic implants offered first insights into osteoblast physiology and mineralization under load, and a large amount of general research has identified some of the critical steps of osteoblast reactions in response to mechanical load.[35,37,53,54] A threshold of tolerated micromotion has been identified, somewhere between 500 and 3,000 με,[37] that leads to anabolic bone regeneration.

The results of the present study indicate that immediate loading of specially designed screw-type implants does not lead to disruption of the implant/bone interface. There is a lack of agreement as to why bone loss occurs during the early healing phase and during function.[55] Surgical trauma has been regarded as one of the most commonly suspected etiologies proposed for early implant failure,[56] but signs of bone loss are not commonly observed after implant surgery.[14] In 1984, Eriksson and Albrektsson reported that the critical temperature for implant site preparation was 47°C for 1 minute or 40°C for 7 minutes.[57] When the bone is overheated, risk of implant failure is significantly increased. Overheating may be generated by excessive pressure at the crestal region during implant surgery. Matthews and Hirsch demonstrated that temperature elevation was influenced more by the force applied than drill speed.[58] However, it was found that when both drill speed and applied force were increased, no significant increase in temperature was observed due to efficient cutting.[58,59] Some studies indicate that screw-type implants placed using a modified minimally traumatizing technique[60] have been osseointegrated.[61]

Signs of tissue necrosis were not observed in the present study by SEM and TEM. An atraumatic surgical technique (high-speed bur, moderate pressure) may be responsible for the observed results. A screw-type implant design, as in the case of osteosynthesis screws, enhanced a direct primary bone/implant contact over the whole implant surface. The present results are in agreement with the findings of Rubin and McLeod, who demonstrated that exposure to low-amplitude mechanical strains can enhance the biologic fixation of implants.[62] Additionally, the success of functionally stable osteosynthesis systems indicates that load can be transferred immediately to osteosynthesis screws without loosening the screw/bone interface. In this study, osteoblasts were found to be intimately attached to the implant surface even when occlusal loads were applied. Stable bone/implant contacts were observed at the implant surface over a 14-day loading period in both groups. The firm attachment of osteoblasts to the implant surface was a characteristic finding observed from the first day following exposure to the artificial substrate. Osteoblasts were able to accommodate their cell bodies in the minigrooves placed in the neck and tip area of the implants. Minigrooves were manufactured in these areas in an attempt to improve bone formation and to enhance the overall surface area of implants. That minigrooves have the ability to enhance formation of bone-like tissue in vivo and in vitro has been demonstrated by Chehroudi and coworkers.[63,64]

The present study revealed that osteoblast adhesion to the implant surface was unimpaired, even when implants were loaded by vertical occlusal forces. At the ultrastructural level, the attached cells displayed all features of active cell function. The bony tissue, which consisted of both cells and mineralized extracellular matrix, was not detached from the implant material, indicating a direct bond without adverse motions between bone and implant.

Most studies on bone deformation have described micromotion in terms of a distance (μm) and not in the biologic term με. The term *micromovement* is widely used in the literature, but has not been well described. Only a few studies have tried to measure micromovement directly in the bony layer adjacent to the implant side, while most studies on this issue have assessed micromotion at a nearer or further distance from the implant placement site.

Cameron and associates found that limited micromotion does not prevent bone ingrowth; on the other hand, motions of approximately 200 μm resulted in fibrous tissue integration instead of bone ingrowth.[65,66] Tolerance to micromotion was also observed by Maniatopoulos and coworkers.[67] Mastication following implantation was allowed immediately and led to implant micromotions via the periodontal ligament estimated to be in the 30-μm range.[68] The authors found that after 3 months, porous cylinders were osseointegrated, while screws were encapsulated by a fibrous membrane.

Their observations suggest that micromotion does not systematically lead to fibrous tissue interposition and that tolerance to micromotion is design- and/or surface-dependent. In a controlled micromotion model in the dog mandible, Pilliar and colleagues showed that micromotions of up to 50 µm were tolerated for porous conical cylinders.[69] The threshold of tolerated micromotion was found to be higher than 30 µm, the previously assumed threshold.[68] In a different controlled micromotion model, Soballe and coworkers showed that micromotions of 150 µm were tolerated by calcium phosphate (CaP) –coated titanium alloy (TiAIV) implants.[70,71] Under the same loading conditions, plasma-sprayed TiAIV implants (without the CaP layer) were encapsulated in fibrous tissue. When submitted to 500-µm micromotion, the CaP-coated and non-coated TiAIV implants failed to osseointegrate.[70] The authors showed that the threshold level of tolerated micromotion lies between 50 and 150 µm for roughened bioinert surfaces. This and other studies have suggested that the presence of a CaP layer appeared to enhance tolerance toward micromotion.[16,71–75]

In the case of dental implants, it is of major importance for the bone-forming osteoblasts to not only attach to the surface, but also to rapidly deposit mineralized matrix on the surface of (or in close apposition to) newly implanted material. This swift deposition of bone is assumed to supply mechanical stability to the implant, thus minimizing motion-induced damage to the tissue at the implantation site.

The present study demonstrated formation of a bone-like mineral over the whole length of the implant. SEM and TEM investigations revealed a direct bond between regularly mineralized collagen fibers and the titanium surface. A fracturing of the implant-containing alveolar bone showed that the strength of the implant/bone bond seemed to be in the same range as the bone matrix bond itself. These findings are in accordance with the results of Rubin and McLeod, who found a promotion of bony ingrowth in titanium alloy cylinders by frequency-specific, low-amplitude mechanical strain.[62] A theoretical model for the role of strain energy density in the initial mineralization of collagen tissues was presented by Harrigan and Reuben and used to derive a limit for the allowable strain magnitudes in tissue-engineered biomaterials.[76] Their model incorporated the mechanical energy in calcified tissue as time-varying loads introduced in energetic arguments for mineralization. This approach has ameliorated the prediction of strains critical for the mineralization of calcifying biologic tissues.

Mineral formation at the implant site, as found in the present study, may result from a low strain level at the implant surface. Implant healing is often compared to bone fracture healing. This is because micromotions are known to positively influence bone fracture healing, and the same may be relevant for implant healing. It has been reported by Joos and associates that optimal healing is achieved not in the total absence of micromotion but in a distinct mechanical environment that accelerates the process of fracture healing.[77] Bone submitted to cyclic micromovements elicits a more physiologic pattern of tissue regeneration than bone not being stimulated mechanically. Thus, the early loading of dental implants seems to function as a mechanical stimulus for osteoblasts.[78]

CONCLUSIONS

The results of this study indicate that immediate loading of biomimetically designed implants can be performed without disturbance of the early osseointegration process in the minipig model. Cell adhesion and direct mineral apposition were present at the whole implant surface under estimated bone strains lower than 5,000 µε. Bone formation at the implant surface may directly reflect the micromovement below the critical strain level. Further studies are necessary to evaluate quantitatively the bone response at implant surfaces under various load applications and to investigate the long-term outcome of immediate loaded dental implants in a clinical setting.

REFERENCES

1. Adell R, Eriksson B, Lekholm U, Brånemark P-I, Jemt T. A long-term follow-up study of osseointegrated implants in the treatment of totally edentulous jaws. Int J Oral Maxillofac Implants 1990;5:347–359.
2. Adell R, Lekholm U, Grøndahl K, Brånemark P-I, Lindström J, Jacobsson M. Reconstruction of severely resorbed edentulous maxillae using osseointegrated fixtures in immediate autogenous bone grafts. Int J Oral Maxillofac Implants 1990;5:233–246.
3. Friberg B, Jemt T, Lekholm U. Early failures in 4,641 consecutively placed Brånemark dental implants: A study from stage I surgery to the connection of completed prostheses. Int J Oral Maxillofac Implants 1991;6:142–146.
4. Brånemark P-I, Hansson BO, Adell R, et al. Osseointegrated implants in the treatment of the edentulous jaw. Experience from a 10-year period. Scand J Plast Reconstr Surg 1977;16:1–132.
5. Adell R, Lekholm U, Rockler B, Brånemark P-I. A 15-year study of ossseointegrated implants in the treatment of the edentulous jaw. Int J Oral Surg 1981;10:387–416.

6. Zarb GA, Jansson T. Prosthodontic procedures. In: Brånemark P-I, Zarb GA, Albrektsson T (eds). Tissue-integrated Prostheses: Osseointegration in Clinical Dentistry. Chicago: Quintessence, 1985:241–282.
7. Albrektsson T, Hansson T, Lekholm U. Osseointegrated dental implants. Dent Clin North Am 1986;30:151–174.
8. Albrektsson T, Brånemark P-I, Hansson HA, Lindström J. Osseointegrated titanium implants: Requirements for ensuring a long-lasting, direct bone to implant anchorage in man. Acta Orthop Scand 1981;52:155–170.
9. Brånemark P-I. Osseointegration and its experimental background. J Prosthet Dent 1983;50:399–410.
10. Roberts WE, Smith RK, Zilberman Y, Mozsary PG, Smith RS. Osseous adaptation to continuous loading of rigid endosseous implants. Am J Orthod 1984;86:30–42.
11. Roberts WE, Garetto LP, De Castro RA. Remodeling of devitalized bone threatens periosteal margin integrity of endosseous titanium implants with threaded or smooth surfaces: Indications for provisional loading and axially directed occlusion. J Indiana Dent Assoc 1989;68:19–24.
12. Zreiqat H, Crotti TN, Howlett CR, Capone M, Markovic B, Haynes DR. Prosthetic particles modify the expression of bone-related proteins by human osteoblastic cells in vitro. Biomaterials 2003;24:337–346.
13. Ghalambor N, Cho DR, Goldring SR, Nihal A, Trepman E. Microscopic metallic wear and tissue response in failed titanium hallux metatarsophalangeal implants: Two cases. Foot Ankle Int 2002;23:158–162.
14. Deporter DA, Watson PA, Pilliar RM, et al. A histological assessment of the initial healing response adjacent to porous surfaced Ti alloy dental implants in dogs. J Dent Res 1986;65:1064–1070.
15. Hashimoto M, Akagawa Y, Hashimoto N, Nikai H, Tsuru H. Single crystal sapphire endosseous implant loaded with functional stress: Clinical and histological evaluation of peri-implant tissues. J Oral Rehabil 1988;15:65–76.
16. Lum LB, Beirne OR, Curtis DA. Histological evaluation of Ha-coated vs uncoated titanium blade implants in delayed and immediately loaded applications. Int J Oral Maxillofac Implants 1991;6:456–462.
17. Akagawa Y, Ichikawa Y, Nikai H, Tsuru H. Interface histology of early loaded partially stabilized zirconia endosseous implant in initial bone healing. J Prosthet Dent 1993;69:599–604.
18. Piattelli A, Ruggierie A, Franchi M, Romasco N, Trisi P. A histologic and histomorphometric study of bone reactions to unloaded and loaded non-submerged single implants in monkeys: A pilot study. J Oral Implantol 1993;19:314–320.
19. Sagara M, Akagawa Y, Nikai H, Tsuru H. The effects of early occlusal loading on one-stage titanium implants in beagle dogs: A pilot study. J Prosthet Dent 1993;69:281–288.
20. Piattelli A, Paolantonio M, Corigliano M, Scarano A. Immediate loading of titanium plasma-sprayed screw-shaped implants in man: A clinical and histological report of 2 cases. J Periodontol 1997;68:591–597.
21. Corso M, Sirota C, Fiorellini J, Rasool F, Szmukler-Moncler S, Weber H-P. Evaluation of the osseointegration of early loaded free-standing dental implants with various coatings in the dog model: Periotest and radiographic results. J Prosthet Dent 1999;82:428–435.
22. Szmukler-Moncler S, Salama S, Reingewirtz Y, Dubruille J-H. Timing of loading and effect of micro-motion on bone-implant interface: A review of experimental literature. J Biomed Mater Res 1998;43:193–203.
23. Linkow LI, Donath K, Lemmons JE. Retrieved analysis of a blade implant after 231 months of clinical function. Implant Dent 1992;1:37–43.
24. Brunski JB. In vivo bone response to biomechanical loading at the bone/dental-implant interface. Adv Dent Res 1999;13:99–119.
25. Brunski JB, Puleo DA, Nanci A. Biomaterials and biomechanics of oral and maxillofacial implants: Current status and future developments. Int J Oral Maxillofac Implants 2000;15:15–46.
26. Stanford CM. Biomechanical and functional behavior of implants. Adv Dent Res 1999;13:88–92.
27. Stanford CM, Brand RA. Toward an understanding of implant occlusion and strain-adaptive bone modeling and remodeling. J Prosthet Dent 1999;81:553–561.
28. Hoshaw SJ, Brunski JB, Cochran GVB. Mechanical loading of Brånemark implants affects interfacial bone modeling and remodeling. Int J Oral Maxillofac Implants 1994;9:345–360.
29. Quirynen M, Naert I, van Steenberghe D. Fixture design and overload influence marginal bone loss and fixture success in the Brånemark System. Clin Oral Implants Res 1992;3:104–111.
30. Isidor F. Loss of osseointegration caused by occlusal load of oral implants. A clinical and radiographic study in monkeys. Clin Oral Implants Res 1996;7:143–152.
31. Isidor F. Histological evaluation of peri-implant bone at implants subjected to occlusal overload or plaque accumulation. Clin Oral Implants Res 1997;8:1–9.
32. Wehrbein H, Glatzmaier J, Yildirim M. Orthodontic anchorage capacity of short titanium screw implants in the maxilla. An experimental study in the dog. Clin Oral Implants Res 1997;8:131–141.
33. Wehrbein H, Merz BR, Hämmerle CHF, Lang NP. Bone-to-implant contact of orthodontic implants in humans subjected to horizontal loading. Clin Oral Implants Res 1998;9:348–353.
34. Gotfredsen K, Berglundh T, Lindhe J. Bone reactions adjacent to titanium implants subjected to static load. A study in the dog (1). Clin Oral Implants Res 2001;12:1–8.
35. Lanyon LE. Functional strain as a determinant for bone remodeling. Calcif Tissue Int 1984;36:56–61.
36. Meyer U, Wiesmann HP, Meyer T, et al. Microstructural investigations of strain-related collagen mineralization. Br J Oral Maxillofac Surg 2001;39:381–389.
37. Frost HM. Mechanical determinants of bone remodeling. Metab Bone Dis Relat Res 1982;4:217–229.
38. Pierrisnard L, Hure G, Barquins M, Chappard D. Two dental implants designed for immediate loading: A finite element analysis. Int J Oral Maxillofac Implants 2002;17:353–362.
39. Meyer U, Vollmer D, Bourauel C, Joos U. Sensitivity analysis of bone geometries around oral implants upon bone loading using finite element method. Comp Meth Biomech Biomed Eng 2001;3:553–559.
40. Joos U, Vollmer D, Kleinheinz J. Effect of implant geometry on strain distribution in peri-implant bone. Mund Kiefer Gesichtschir 2000;4:143–147.
41. Meyer U, Meyer T, Jones DB. Attachment kinetics, proliferation rates and vinculin assembly of bovine osteoblasts cultured on different pre-coated artificial substrates. J Mater Sci Mater Med 1998;9:301–307.
42. Buser D, Nydegger T, Hirt HP, Cochran DL, Nolte LP. Removal torque values of titanium implants in the maxilla of miniature pigs. Int J Oral Maxillofac Implants 1998;13:611–619.

43. Plate U, Arnold S, Stratmann U, Wiesmann HP, Höhling HJ. General principle of ordered apaptitic crystal formation in enamel and collagen rich hard tissues. Connect Tissue Res 1998;38:149–157.
44. Kossovsky N. It's a great new material, but will the body accept it? Res Dev 1989;3:48–54.
45. Ratner BD. Society for Biomaterials 1992 Presidential Address: New ideas in biomaterials science—A path to engineered biomaterials. J Biomed Mater Res 1993;27:837–850.
46. Borchers L, Reichart P. Three-dimensional stress distribution around a dental implant at different stages of interface development. J Dent Res 1983;62:155–159.
47. Mihalko WM, May TC, Kay JF, Krause WR. Finite element analysis of interface geometry effects on the crestal bone surrounding a dental implant. Implant Dent 1992 Fall;1(3):212–217.
48. Papavasiliou G, Kamposiora P, Bayne SC, Felton DA. Three-dimensional finite element analysis of stress distribution around single tooth implants as a function of bony support, prosthesis type, and loading during function. J Prosthet Dent 1996;76:633–640.
49. Soltész U, Siegele D. Einfluß der Steifigkeit des Implantmaterials auf die in Knochen erzeugten Spannungen. Dtsch Zahnärztl Z 1984;39:183–186.
50. Meyer U, Vollmer D, Runte C, Bourauel C, Joos U. Bone loading pattern around implants in average and atrophic edentulous maxillae: A finite element analysis. J Craniomaxillofac Surg 2001;29:100–105.
51. Benzing UR, Gall H, Weber H. Biomechanical aspects of two different implant-prosthetic concepts for edentulous maxillae. Int J Oral Maxillofac Implants 1995;10:188–198.
52. Meyer U, Vollmer D, Homann C, et al. Experimentelle und Finite-Element-Analyse der Biomechanik des Unterkiefers unter Belastung. Mund Kiefer Gesichtschir 2000;4:14–20.
53. Galante J, Rostoker W, Leuck R, Ray RD. Sintered fiber metal composites as a basic for attachment of implants to bone. J Bone Joint Surg 1971;53:101–114.
54. Meyer U, Wiesmann HP, Kruse-Lösler B, Handschel J, Stratmann U, Joos U. Strain-related bone remodeling in distraction osteogenesis of the mandible. Plast Reconstr Surg 1999;103:800–807.
55. Oh T-J, Yoon J, Misch CE, Wang H-L. The causes of early implant bone loss: Myth or science? J Periodontol 2002;73:322–333.
56. Esposito M, Hirsch JM, Lekholm U, Thomsen P. Biological factors contributing to failures of osseointegrated oral implants. (II). Etiopathogenesis. Eur J Oral Sci 1998;106:721–764.
57. Eriksson RA, Albrektsson T. The effect of heat on bone regeneration. J Oral Maxillofac Surg 1984;42:701–711.
58. Matthews L, Hirsch C. Temperatures measured in human cortical bone when drilling. J Bone Joint Surg 1972;54:297–308.
59. Brisman DL. The effect of speed, pressure, and time on bone temperature during the drilling of implant sites. Int J Oral Maxillofac Implants 1996;11:35–37.
60. Benington IC, Biagioni PA, Briggs J, Sheridan S, Lamey PJ. Thermal changes observed at implant sites during internal and external irrigation. Clin Oral Implants Res 2002;13:293–297.
61. Albrektsson T, Johansson C. Osteoinduction, osteoconduction and osseointegration. Eur Spine J 2001;10:96–101.
62. Rubin CT, McLeod KJ. Promotion of bony ingrowth by frequency-specific, low-amplitude mechanical strain. Clin Orthop 1994;298:165–174.
63. Chehroudi B, McDonnell D, Brunette DM. The effects of micromachined surfaces on formation of bonelike tissue on subcutaneous implants as assessed by radiography and computer image processing. J Biomed Mater Res 1997;34:279–290.
64. Chehroudi B, Ratkay J, Brunette DM. The role of surface geometry on mineralization in vitro and in vivo: A transmission and scanning electron microscope study. Cells Mater 1992;2:89–104.
65. Cameron H, Pilliar RM, Macnab I. Porous surfaced vitallium staples. S Afr J Surg 1972;10:63–70.
66. Cameron H, Pilliar RM, Macnab I. The effect of movement on the bonding of porous metal to bone. J Biomed Mater Res 1973;7:301–311.
67. Maniatopoulos C, Pilliar RM, Smith D. Threaded versus porous-surfaced designs for implant stabilization in bone-endodontic implant model. J Biomed Mater Res 1986;20:1309–1333.
68. Pilliar RM. Quantitative evaluation of the effect of movement at a porous coated implant-bone interface. In: Davies JE, Albrektsson T (eds). The Bone-Biomaterial Interface. Toronto: University of Toronto Press, 1991:380–387.
69. Pilliar RM, Deporter D, Watson PA. Tissue-implant interface: Micro-movements effects. In: Vincenzini P (ed). Advances in Science and Technology. Vol 12: Materials in clinical applications. Faenza: Techna, 1995:569–579.
70. Soballe K, Hansen ES, Brockstedt-Rasmussen H, Bünger C. Tissue ingrowth into titanium and hydroxyapatite coated implants during stable and unstable mechanical conditions. J Orthop Res 1992;10:285–299.
71. Soballe K, Hansen ES, Brockstedt-Rasmussen H, Bünger C. The effects of osteoporosis, bone deficiency, bone grafting and micromotion on fixation of porous-coated hydroxyapatite-coated implants. In: Geesink RGT, Manley MT (eds). Hydroxyapatite Coatings in Orthopaedic Surgery. New York: Raven Press, 1993:107–136.
72. Geesink RGT, de Groot K, Klein CPAT. Chemical implant fixation using hydroxyapatite coating. The development of a human hip prosthesis for chemical fixation to bone using hydroxyapatite coatings on titanium substrates. Clin Orthop Rel Res 1987;225:147–170.
73. Oonishi H, Noda T, Ito S, et al. Effects of hydroxyapatite coating on bone growth into porous titanium implants under loading conditions. J Appl Biomater 1994;5:23–37.
74. Thomas KA, Cook SD, Haddad RJ, Kay JF, Jarcho M. Biological response to hydroxyapatite-coated titanium hips. J Arthroplasty 1989;4:43–53.
75. Szmukler-Moncler S, Reingewirtz Y, Weber H-P. Bone response to early loading: The effect of surface state. In: Davidovitch Z, Norton LA (eds). Biological Mechanisms of Tooth Movement and Craniofacial Adaptation. Boston: Harvard Society for the Advancement of Orthodontics, 1996:611–616.
76. Harrigan TP, Reuben JD. Mechanical model for critical strain in mineralizing biological tissues: Application to bone formation in biomaterials. Biomaterials 1997;18:877–883.
77. Joos U, Piffko J, Meyer U. New aspects in managing mandibular fractures. Mund Kiefer Gesichtschir 2001;5:2–16.
78. Misch CE, Bidez MW, Sharawy M. A bioengineered implant for a predetermined bone cellular response to loading forces. A literature review and case report. J Periodontol 2001;72:1276–1286.